Journal of the Korean Chemical Society
2018, *Vol. 62, No. 2*
Printed in the Republic of Korea
https://doi.org/10.5012/jkcs.2018.62.2.106

Evaluation of Thermal Hysteresis Activity of Ice-binding Proteins Using Ice-etching and Molecular Docking

Wahyu Sri Kunto Nugroho[†], Sangwook Wu[‡], and Hak Jun Kim[†,*]

[†]*Department of Chemistry, Pukyong National University, Busan 48513, Korea.* [*]*E-mail: kimhj@pknu.ac.kr*
[‡]*Department of Physics, Pukyong National University, Busan 48513, Korea.*

(Received January 2, 2018; Accepted February 14, 2018)

ABSTRACT. Ice-binding proteins have an affinity for ice. They create a gap between the melting and freezing points by inhibiting the growth of ice, known as thermal hysteresis (TH). Interestingly, moderately active LeIBP and hyperactive FfIBP are almost identical in primary and tertiary structures, but differ in TH activity. The TH of FfIBP is tenfold higher than that of LeIBP, due to a subtle difference in their ice-binding motifs. To further evaluate the difference in TH, the interactions were investigated by ice-etching and molecular docking. Ice-etching showed that FfIBP binds to the primary and secondary prism, pyramidal, and basal planes; previously, LeIBP was found to bind to the basal and primary prism planes. Docking analysis using shape complementarity (*Sc*) showed that the hyperactive FfIBP had higher *Sc* values for all four ice planes than LeIBP, which is comparable with TH. Docking can be used to describe the hyperactivity of IBPs.

Key words: Ice-binding protein, Thermal hysteresis, Ice crystal planes, Docking, Shape complementarity

INTRODUCTION

Ice-binding proteins (IBPs) are a group of proteins with an affinity for ice, such as the antifreeze proteins (AFPs) and ice-nucleating proteins.[1–3] IBPs are essential for the survival of many psychrophiles in sub-zero environments.[2,4–6] IBPs are able to bind to and inhibit the growth of the ice, lowering the freezing point of the solution.[1,2,7] As a result, IBPs create a gap between the melting and freezing points of a solution. This difference is called thermal hysteresis (TH), which is a quantitative measure of the activity of IBPs.[7,8] AFPs are a subset of IBPs and have TH activity.[9] Based on their TH activities, IBPs can be classified as moderately-active (less than 1.0 °C) and hyperactive IBPs (greater than 1.0 °C).[10–12] It is hypothesized that the difference in TH may result from the interaction between IBPs and specific ice crystal planes, and additionally, the area of interaction between the two.[2,13–21] Therefore, the difference should be reflected in their primary and tertiary structures.[1,2,8] Various IBPs have diverse structures but have relatively common ice-binding sites (IBSs), which are flat and rigid hydrophobic regions.[2,8,22] Hydrophobicity is known to play a critical role in ordering hydrated water molecules into ice-like arrangements,[23,24] while the flatness of IBSs appears to be the ideal geometrical fit for the specific ice planes.[25] Notably, an interaction between ice crystal planes and IBPs modifies the ice morphology, which is maintained within the hysteresis gap in an IBP-specific manner.[1,26,27]

The ice crystal structure depends on the temperature and pressure at which ice crystals are formed.[28] However, the most stable ice crystal under ambient pressures at ± 0 °C is a hexagonal ice crystal (Ice Ih) (*Fig.* 1). Ice Ih has a $P6_3/mmc$ space group with the cell dimensions a = b = 4.49749 Å and c = 7.322382 Å, α = β = 90°, γ =120°.[29] Ice Ih is a symmetrical ice crystal structure; the "c-axis" is the main hexagonal symmetrical axis, and the three "a-axis" are perpendicular to the "c-axis".[30] Although multiple ice planes can be generated from Ice Ih, only limited ice planes appear during the measurement of an IBP's activity, such as the primary prism, secondary prism, pyramidal, and basal planes (*Fig.* 1). This means that IBPs can bind to the specific ice planes during the growth of ice.[13] Experimental evidence supporting the interaction between ice and IBPs was first reported by Knight.[14] In the ice-etching method, IBPs bound to the specific ice planes of a hemisphere single ice crystal leaves etching pattern during and after evaporation.[14] The ice-etching experiment revealed that type I fish AFPs from winter flounder (*Pseudopleuronectes americanus*) and Alaskan plaice (*Pleuronectes quadritaberulatus*) adsorb onto the pyramidal planes of ice, whereas the type I AFP from the Sculpin (*Myoxocephalus scorpius*) adsorbs onto the secondary prism planes.[14] Furthermore, a few IBPs seem to bind to different ice crystal planes simultaneously: type III fish AFP and AFP from the Antarctic bacterium *Colwellia* sp. strain SLW05 (ColAFP) bind to both a primary prism and pyramidal planes of ice.[31–33] These findings suggest that

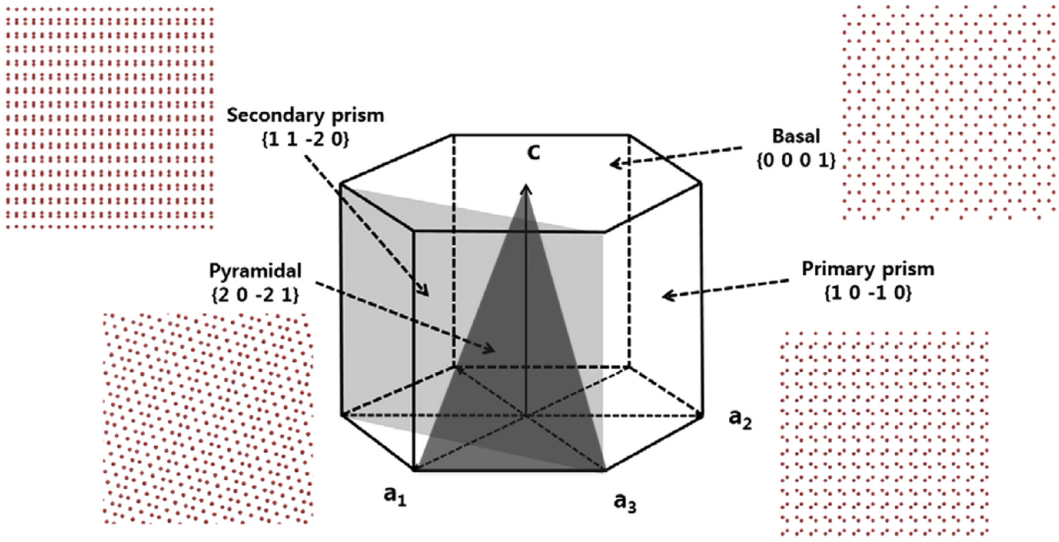

***Figure* 1.** Hexagonal unit cell of an ice crystal (Ih) and ice planes docked with IBPs in the present study. The secondary prism is shaded in light gray and pyramidal plane in dark gray.

each IBP has a unique ice-binding mechanism, either moderately active or hyperactive.

Recently, our group has isolated two structurally similar IBPs: one, designated as LeIBP, from Arctic yeast, *Glaciozyma* sp.,[34] and the other, designated as FfIBP, from the sea ice bacterium, *Flavobacterium frigoris*.[35] Intriguingly, the two IBPs exhibited severely different TH activity, despite their high sequence identity (56%) and similar tertiary β-helical structures (*Fig.* 2). The β-helical structure is common in hyperactive insect, fungal, and bacterial AFPs or IBPs.[19]

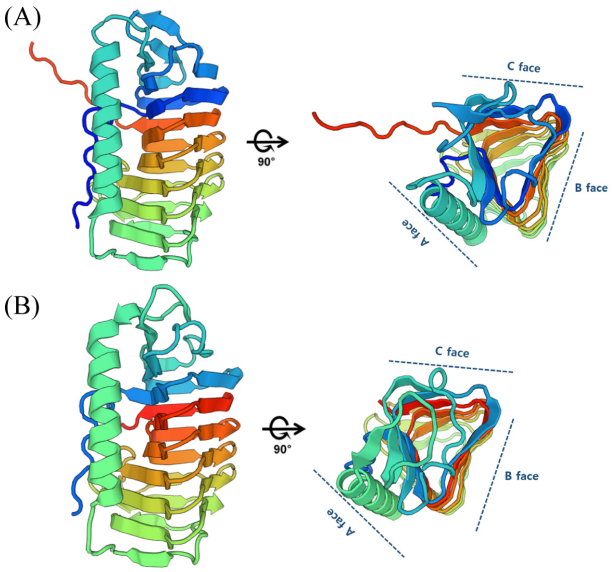

***Figure* 2.** Ribbon diagram of trigonal cylindrical structures of (A) LeIBP (PDB ID: 3UYV) and (B) FfIBP (PDB ID: 4NU2).

Generally, β-sheets of insect AFPs contain a regular and repetitive T-X-T ice-binding motif, which help the AFPs bind onto ice planes.[11] However, LeIBP, FfIBP, ColAFP, and *Thypula ishikariensis* AFP (TisAFP) have no such distinct ice-binding motif, but FfIBP has a relatively unique ice-binding motif (T-A/G-X-T/N motif) compared to LeIBP, ColAFP, and TisAFP.[18,35] The TH activity of FfIBP was almost tenfold higher than that of LeIBP at the same molar concentration; TH values of FfIBP and LeIBP were 2.5 °C at 50 μM and ca 0.34 °C at 430 μM, respectively.[17,35] We speculate that this difference might result from the relative regularity of the ice-binding motif and interaction of the IBP with specific ice planes. Previously, LeIBP was shown to bind to basal and primary prism planes,[17] but recognition of ice planes by FfIBP has not been experimentally investigated.

In order to gain better insight into the different TH activities of the two IBPs, we conducted an ice-etching experiment with FfIBP, and analyzed the interaction between the IBPs and ice planes using the docking program Hex. Using the docking program, we can calculate and find the lowest energy of interaction between IBPs and ice planes. Then, the conformation of interacting IBPs and ice planes was further evaluated by calculating the degree of fitness (complementarity) between the two surfaces. A higher degree of shape complementarity (*Sc*) between two surfaces is expected to possess stronger interactions. Here, we attempt to provide insight into the TH difference between two structurally similar IBPs by comparing the TH, ice-etching, and docking results.

EXPERIMENTAL

Expression and Purification of Recombinant FfIBP

The recombinant FfIBP was expressed and purified as described previously.[35] Briefly, the *E. coli* BL21 strain, harboring the FfIBP gene in the pColdI vector, was grown at 37 °C in Luria-Bertani (LB) medium containing 100 μg/ml ampicillin with shaking until the OD_{600} reached 0.6. Then, the bacterial culture was transferred to 15 °C and further incubated for 1 h. The recombinant FfIBP was induced by adding isopropyl beta-D-thiogalactopyranoside to a final concentration of 1 mM, and the cells were further incubated at 15 °C for 20 h. The harvested cell pellet was resuspended and incubated for 30 min in 50 mM sodium phosphate pH 8.5, 300 mM NaCl, 5 mM imidazole, 0.5 mg/ml lysozyme, and 1 mM phenylmethylsulfonyl fluoride. The cell suspension was disrupted by ultrasonication (Vibra-Cell VCX400) and centrifuged at 12,000 rpm for 1 h at 4 °C. The supernatant was loaded onto a His-tag affinity column. The column was washed with ten column volumes of lysis buffer and eluted with 50 mM sodium phosphate pH 8.5, 300 mM NaCl, 300 mM imidazole. The eluent, containing FfIBP, was dialyzed against the lysis buffer. The concentration of FfIBP was determined using UV spectrophotometry with an extinction coefficient at 280 nm of 26930 M^{-1} cm^{-1}.

Ice-etching Experiment of FfIBP

Single ice crystal preparation and the ice-etching experiment were performed as described elsewhere with slight modification.[14] A single ice crystal (2.5 cm × 2.5 cm × 2.5 cm) was mounted to the cold-finger to the long axis, of which either the basal or primary prism planes of the ice crystal were oriented. The mounted ice crystal was placed into degassed water (4 °C), and the temperature of the cold-finger was lowered and maintained at -7 °C for 3 h by circulating a coolant. In this stage, the ice crystal was grown into the ice hemisphere. Then, the ice hemisphere was dipped into the IBP-containing solution (1~5 μM), and the cold-finger was cooled and maintained for 30 min at -10 °C. The FfIBP-bound ice hemisphere was detached from the cold-finger and transferred to a cold room at -10 °C. To expose the distinct etching pattern, the surface of the ice hemisphere was scraped briefly using a sharp blade and left to evaporate for at least 1 h.

Docking Study

LeIBP (PDB ID: 3UYV) and FfIBP (PDB ID: 4NU2) structural files were obtained from RCSB PDB (www.rcsb.org). Four types of ice crystal planes, i.e.: the primary prism {1 -1 0 0}, secondary prism {2 -1 -1 0}, pyramidal {1 -1 0 1}, and basal {0 0 0 1} planes, were generated by VESTA software, version 3.2.1.[36] The interaction poses between IBPs and those ice crystals were searched using the Hex 8.0 docking program.[37] Default parameters of Hex 8.0 were used, except for the correlation type (Shape + Electrostatic), post-processing (OPLS Minimisation), and final search (30). The best predicted conformations were saved, and the shape complementarities (*Sc*) were calculated using the *SC* program in the CCP4 program suite.[38]

RESULTS AND DISCUSSION

Ice-etching Patterns Showed that FfIBP Bound to Multiple Ice Planes

A single ice hemisphere, whose either basal plane or primary prism plane was oriented normal to the finger, was immersed in a FfIBP-containing solution, as shown in *Fig*. 3. There was no unique ice-etching pattern formed by FfIBP, regardless of the ice crystal orientation (*Fig*. 3A and B), indicating that it binds to the entire surface of the ice hemisphere. A handful of data showed that absorption of IBPs onto the multiple ice planes seems to be mediated by their compound IBSs.[31,33,39] Mutagenesis and GFP-tagging of moderately active fish type III AFP variant QAE revealed it binds to both primary and pyramidal ice planes by two

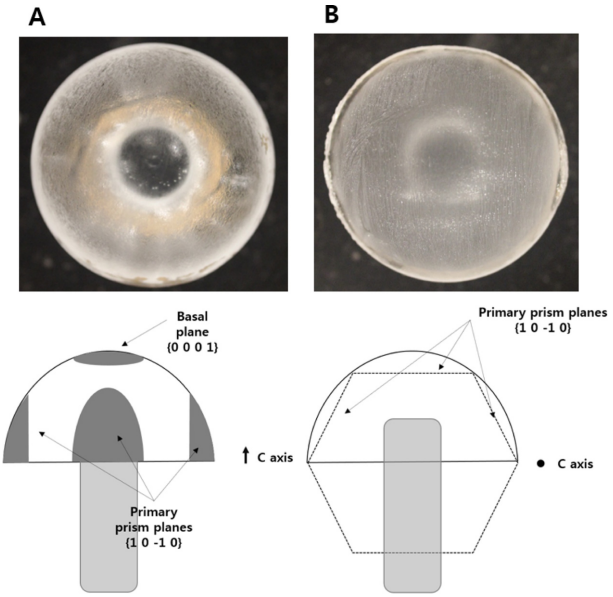

***Figure* 3.** Ice etching photographs of FfIBP. Top view (upper panel) of a single ice crystal hemisphere grown in a FfIBP-containing solution with its c-axis parallel (A) or normal (B) to the cold-finger. (Lower panel) Schematic drawing (lower panel) of each hemisphere grown with its c-axis parallel (A) or normal to (B) the cold-finger. In the right panel, the shaded areas are the basal and primary prism planes.

adjacent and flat IBSs forming an angle of 150° from each other. primary, and pyramidal ice plane binding sites forming an angle of 150° from each other, each binding primary and pyramidal ice planes.[31] However, moderately active fish type I AFPs are shown to bind onto only single ice planes: AFPs from winter flounder (*Pseudopleuronectes americanus*) and Alaskan plaice (*Pleuronectes quadritaberulatus*) bound to the pyramidal planes of ice, while the Sculpin (*Myoxocephalus Sc orpius*) AFP to the secondary prism planes.[14] Additionally, hyperactive TisAFP and ColAFP, two closest homologs of FfIBP and LeIBP, also bound to multiple ice planes by two IBSs on the flat β-sheet and the adjacent loop.[33,39] Based on the ice-etching experiments, both LeIBP and FfIBP bound to multiple ice planes, however, it is not clear how many IBSs exist in FfIBP and LeIBP due to the limited site-directed mutagenesis study.

As other hyperactive IBPs, for example ColAFP, hyperactive FfIBP recognized multiple ice planes, such as the basal, primary prism, and secondary prism planes.[11,33,39–44] However, previously we have also shown that even moderately active LeIBP binds, relatively weakly, to the basal and primary prism planes.[17] Since the binding onto the basal plane was hypothesized to be the hallmark of hyperactivity of IBPs,[16,40] the ice-etching observation *per se* may demonstrate that LeIBP may not be moderately active, but hyperactive.[17] On the contrary to this hypothesis, our result indicated that the binding onto the basal plane cannot guarantee the hyperactivity of IBPs. Hence we employed the docking and shape complementarity to further evaluate the strength of the interaction between the IBPs and specific ice planes.

Docking Study May Explain the Difference in TH Activity Between LeIBP and FfIBP

The flatness of the ice binding site (IBS) is considered important for the IBP's function, which provides an ideal geometrical fit to bind ice planes.[22] As shown in *Fig.* 2, LeIBP and FfIBP roughly have 3 faces (A, B, and C faces), which are relatively flat. Mutagenesis revealed that the IBSs of LeIBP and FfIBP are on the B faces.[19]

In order to gain better insight into the interactions of LeIBP and FfIBP with ice, docking was performed to acquire the lowest energy interactions between the IBPs and the ice crystals using Hex 8.0 docking software, with the parameters listed in Materials and Methods. The B-face of each IBP was docked onto the four ice crystal planes: the primary prism, secondary prism, pyramidal, and basal planes. The shape complementarity (*Sc*) of the lowest energy interactions between IBPs and the ice crystals were then calculated to evaluate the interaction of the IBP and ice planes (*Table* 1).

***Table* 1.** *Sc* values of the interactions between B faces of the IBPs and four ice planes

Protein	Ice planes	*Sc*	Contact area (Å^2)
Lysozyme	primary prism	0.27	322.2
LeIBP without water molecules	primary prism	0.41	1045.0
	secondary prism	0.46	817.6
	pyramidal	0.35	1038.5
	basal	0.36	1153.4
LeIBP with water molecules	primary prism	0.45	1093.6
	secondary prism	0.46	809.4
	pyramidal	0.39	1089.0
	basal	0.45	1195.1
FfIBP without water molecules	primary prism	0.47	900.4
	secondary prism	0.45	863.9
	pyramidal	0.53	947.5
	basal	0.46	897.8
FfIBP with water molecules	primary prism	0.49	1040.9
	secondary prism	0.5	1072.7
	pyramidal	0.56	1108.6
	basal	0.5	1052.0

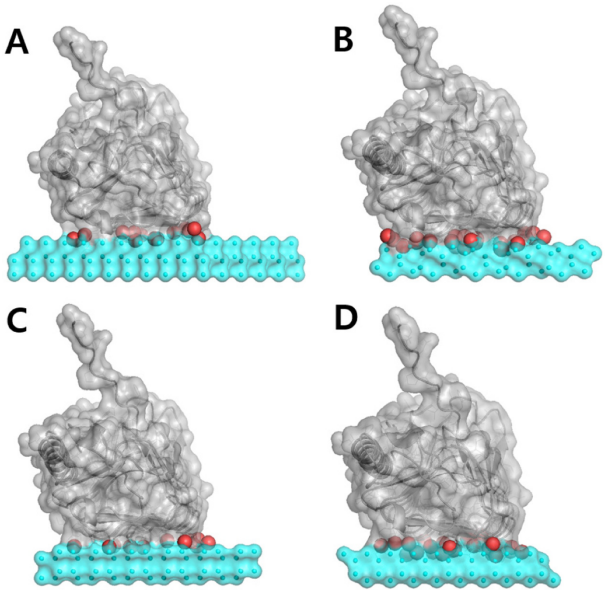

***Figure* 4.** Docking of LeIBP to different ice planes (red spheres are water molecules that contribute directly to binding to the ice crystal). (A) basal, (B) pyramidal (C) primary prism, and (D) secondary prism planes.

A perfect pair of two surfaces has a *Sc* value of 1.0. Generally, IBPs have a *Sc* value between 0.5 and 0.8.[25,33,39] LeIBP and FfIBP interactions with multiple ice planes are shown in the *Figs*. 4 and 5.

Lysozyme (PDB ID: 3A3Q) was used as a control and was docked onto the {1 -1 0 0} primary prism ice plane with a lower *Sc* value (only 0.27). This value agrees with previous

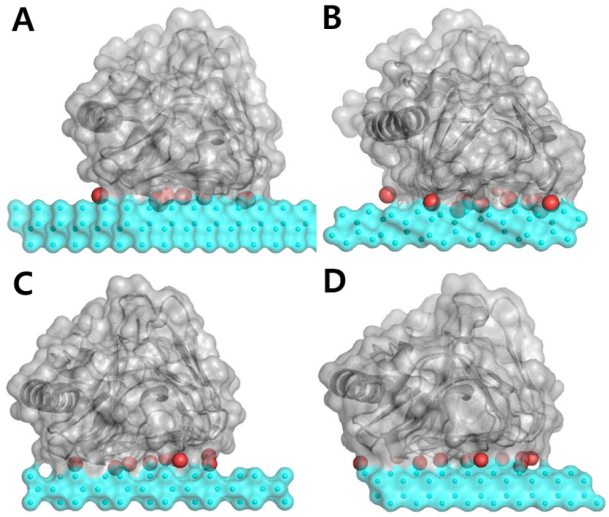

***Figure* 5.** Docking of FfIBP to different ice planes (red spheres are water molecules that contribute directly to binding to the ice crystal). (A) basal, (B) pyramidal (C) primary prism, and (D) secondary prism planes.

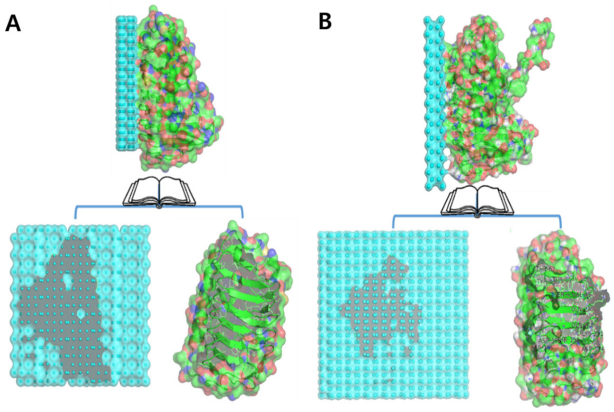

***Figure* 6.** Open book view of interaction between FfIBP and pyramidal plane (A), and between LeIBP and secondary prism plane (B).

results (<0.38).[25,33] This result clearly indicates that the *Sc* value can be used to evaluate the interaction between IBPs and ice. Garnham et al. (2011) showed that bound water molecules on the IBS are directly involved in binding to ice. It was hypothesized that the bound waters relatively regularly embedded in the IBS enable IBPs to bind to ice planes.[24,44] Hence, we removed the water molecules and recalculated the *Sc* values. As shown in *Table* 1, the *Sc* values of IBPs with bound water molecules were higher than those of IBPs without bound water. The result is consistent with prior reports, showing that bound water molecules of a similar arrangement to the ice lattice play an important role in forming a H-bond network with ice.[24,33,39] The present docking study verified that water molecules bound to the IBS of IBPs clearly increase the degree of fitness between IBPs and the specific ice planes.

The calculated *Sc* values of FfIBP in the present study were higher in all cases than those of LeIBP, implying that the IBS of FfIBP has better complementarity to the four ice planes than that of LeIBP. The contact area of the IBS with the primary prism, pyramidal, and basal planes was similar in both IBPs, but that of the IBS with the secondary prism plane was larger in FfIBP (1072.68 Å^2), than in LeIBP (809.39 Å^2). Some of these interactions are displayed in Open book view in *Fig*. 6. A previous report also showed that hyperactive TisAFP8 also had higher *Sc* values than its moderately active counterpart, TisAFP6.[39] The loop region of the hyperactive TisAFP8 had an *Sc* value of 0.55 with contact area of 809.39 Å^2 while that of moderately active TisAFP6 had an of 0.49 with contact area of 783 Å^2. The *Sc* value and contact area were different structurally similar two IBP cases. These differences may lead to the difference in TH activities. Taken together, these data may explain why FfIBP is hyperactive compared to LeIBP.

The *Sc* values can also partly support the observations in the ice-etching experiment. Previously, LeIBP adsorbed preferentially onto the basal, and relatively weakly to the primary prism planes. The docking results indicated that LeIBP with bound water molecules within the IBS additionally binds to the secondary prism plane with a slightly higher *Sc* value than to the basal and primary prism planes (*Table* 1). However, the contact area between the IBS of LeIBP and the secondary prism plane was quite smaller (809.39 Å^2) than those between LeIBP and the primary prism (1093 Å^2) and basal (1195 Å^2) planes. The smaller contact area may account for the no observation of etching pattern of the secondary prism plane in LeIBP, which is consistent with the observation that larger contact surface areas probably compensate for the relatively low *Sc* values.[33] In addition, the interaction between LeIBP and the pyramidal plane was negligible, based on the *Sc* value of 0.39, which is slightly above the values for the non-IBP interaction. The *Sc* value of FfIBP indicates that it binds to all four planes with almost the same values and contact areas, which agrees with the result of the ice-etching experiment. Similarly, the structurally highly similar ColAFP also bound to all four planes with almost the same values.[33] Based on the present observations, the hyperactivity of IBP may be explained by the shape complementarity and contact area between IBS of IBPs and ice crystal, which is intensified by the bound water molecules within IBS. However, the further investigations are needed to answer the difference in TH activity between

structurally similar IBPs.

CONCLUSION

Moderately active LeIBP and hyperactive FfIBP share high structural similarity. The difference in the TH activity between the two IBPs was examined by ice-etching and docking experiments. Ice-etching revealed that hyperactive FfIBP bound to multiple ice planes, while LeIBP bound to the basal and primary prism planes. The docking between the IBS and ice planes was evaluated by calculating the shape complementarity. FfIBP showed better shape complementarity than LeIBP to all four ice planes with larger contact areas. This result agrees with a previous observation of hyperactive AFPs. Taken together, our docking data combined with ice-etching may provide insight into the hyperactivity of IBPs.

Acknowledgments. This work is supported by Pukyong National University (2016).

REFERENCES

1. Kim, H. J.; Lee, J. H.; Hur, Y. B.; Lee, C. W.; Park, S.-H.; Koo, B.-W. *Mar. Drugs*. **2017**, 27.
2. Davies, P. L. *Trends Biochem. Sci.* **2014**, 548.
3. Bar Dolev, M.; Braslavsky, I.; Davies, P. L. *Annu. Rev. Biochem.* **2016**, *85*, 515.
4. Raymond, J. A. *Proc. Natl. Acad. Sci. U.S.A.* **2011**, *108*, E198.
5. Raymond, J. A.; Kim, H. J. *PLoS One* **2012**, *7*, e35968.
6. Raymond, J. A.; Fritsen, C.; Shen, K. *FEMS Microbiol. Ecol.* **2007**, *61*, 214.
7. Kristiansen, E.; Zachariassen, K. E. *Cryobiology* **2005**, *51*, 262.
8. Fletcher, G. L.; Hew, C. L.; Davies, P. L. *Annu. Rev. Physiol.* **2001**, *63*, 359.
9. Lee, S. G.; Lee, J. H.; Kang, S.; Kim, H. J. *Mar. Proteins Pept. Biol. Act. Appl.* **2013**, 667.
10. Graham, L. A.; Liou, Y. C.; Walker, V. K.; Davies, P. L. *Nature* **1997**, *388*, 727.
11. Graether, S. P.; Kuiper, M. J.; Gagne, S. M.; Walker, V. K.; Jia, Z.; Sykes, B. D.; Davies, P. L. *Nature* **2000**, *406*, 325.
12. Hanada, Y.; Kondo, H.; Garnham, C. P.; Togashi, S.; Nishimiya, Y.; Hoshino, T.; Miura, A.; Davies, P. L.; Tsuda, S. In Ice-Binding Protein Conference; Kingston, ON, Canada, 2011.
13. Raymond, J. A.; de Vries, A. L. *Proc. Natl. Acad. Sci. U.S.A.* **1977**, *74*, 2589.
14. Knight, C. A.; Cheng, C. C.; de Vries, A. L. *Biophys. J.* **1991**, *59*, 409.
15. Drori, R.; Celik, Y.; Davies, P. L.; Braslavsky, I. *J. R. Soc. Interface* **2014**, *11*, 20140526.
16. Pertaya, N.; Marshall, C. B.; Celik, Y.; Davies, P. L.; Braslavsky, I. *Biophys. J.* **2008**, *95*, 333.
17. Park, K. S.; Do, H.; Lee, J. H.; Park, S. I.; Kim, E. J.; Kim, S. J.; Kang, S. H.; Kim, H. J. *Cryobiology* **2012**, *64*, 286.
18. Lee, J. H.; Park, A. K.; Do, H.; Park, K. S.; Moh, S. H.; Chi, Y. M.; Kim, H. J. *J. Biol. Chem.* **2012**, *287*, 11460.
19. Do, H.; Kim, S. J.; Kim, H. J.; Lee, J. H. *Acta Crystallogr. D Biol. Crystallogr.* **2014**, *70*, 1061.
20. Nishimiya, Y.; Ohgiya, S.; Tsuda, S. *J. Biol. Chem.* **2003**, *278*, 32307.
21. Baardsnes, J.; Kuiper, M. J.; Davies, P. L. *J. Biol. Chem.* **2003**, *278*, 38942.
22. Jia, Z.; Davies, P. L. *Trends Biochem. Sci.* **2002**, *27*, 101.
23. Nutt, D. R.; Smith, J. C. *J. Am. Chem. Soc.* **2008**, *130*, 13066.
24. Garnham, C. P.; Campbell, R. L.; Davies, P. L. *Proc. Natl. Acad. Sci. U.S.A.* **2011**, *108*, 7363.
25. Leinala, E. K.; Davies, P. L.; Jia, Z. *Structure* **2002**, *10*, 619.
26. Doucet, D.; Tyshenko, M. G.; Kuiper, M. J.; Graether, S. P.; Sykes, B. D.; Daugulis, A. J.; Davies, P. L.; Walker, V. K. *Eur. J. Biochem.* **2000**, *267*, 6082.
27. Graether, S. P.; Slupsky, C. M.; Davies, P. L.; Sykes, B. D. *Biophys. J.* **2001**, *81*, 1677.
28. Bartels-Rausch, T.; Bergeron, V.; Cartwright, J. H. E.; Escribano, R.; Finney, J. L.; Grothe, H.; Gutiérrez, P. J.; Haapala, J.; Kuhs, W. F.; Pettersson, J. B. C. *Rev Mod Phys* **2012**, *84*, 885.
29. Fortes, A. D.; Wood, I. G.; Grigoriev, D.; Alfredsson, M.; Kipfstuhl, S.; Knight, K. S.; Smith, R. I. *J. Chem. Phys.* **2004**, *120*, 11376.
30. Hew, C. L.; Yang, D. S. *Eur. J. Biochem.* **1992**, *203*, 33.
31. Garnham, C. P.; Natarajan, A.; Middleton, A. J.; Kuiper, M. J.; Braslavsky, I.; Davies, P. L. *Biochemistry* **2010**, *49*, 9063.
32. Howard, E. I.; Blakeley, M. P.; Haertlein, M.; Petit-Haertlein, I.; Mitschler, A.; Fisher, S. J.; Cousido-Siah, A.; Salvay, A. G.; Popov, A.; Muller-Dieckmann, C.; Petrova, T.; Podjarny, A. *J. Mol. Recognit.* **2011**, *24*, 724.
33. Hanada, Y.; Nishimiya, Y.; Miura, A.; Tsuda, S.; Kondo, H. *FEBS J.* **2014**, *281*, 3576.
34. Lee, J. K.; Park, K. S.; Park, S.; Park, H.; Song, Y. H.; Kang, S. H.; Kim, H. J. *Cryobiology* **2010**, *60*, 222.
35. Do, H.; Lee, J. H.; Lee, S. G.; Kim, H. J. *Acta Crystallogr. Sect. F Struct. Biol. Cryst. Commun.* **2012**, *68*, 806.
36. Momma, K.; Izumi, F. *J. Appl. Crystallogr.* **2011**, *44*, 1272.
37. Ritchie, D. W.; Venkatraman, V. *Bioinformatics* **2010**, *26*, 2398.
38. Lawrence, M. C.; Colman, P. M. *J. Mol. Biol.* **1993**, *234*, 946.
39. Cheng, J.; Hanada, Y.; Miura, A.; Tsuda, S.; Kondo, H. *Biochem. J.* **2016**, *473*, 4011.
40. Scotter, A. J.; Marshall, C. B.; Graham, L. A.; Gilbert, J. A.; Garnham, C. P.; Davies, P. L. *Cryobiology* **2006**, *53*,

229.
41. Graham, L. A.; Marshall, C. B.; Lin, F. H.; Campbell, R. L.; Davies, P. L. *Biochemistry* **2008**, *47*, 2051.
42. Mok, Y. F.; Lin, F. H.; Graham, L. A.; Celik, Y.; Braslavsky, I.; Davies, P. L. *Biochemistry* **2010**, *49*, 2593.
43. Lin, F. H.; Davies, P. L.; Graham, L. A. *Biochemistry* **2011**, *50*, 4467.
44. Sun, T.; Lin, F. H.; Campbell, R. L.; Allingham, J. S.; Davies, P. L. *Science* **2014**, *343*, 795.